CHARACTERISTIC CONSTRAINT MODES FOR COMPONENT MODE SYNTHESIS

Course Project Report

ME-6106

Computational Structural Dynamics

by

R. NITIN IYER
(ROLL NO: 19310R001)

Under the Guidance of

Prof. Salil S. Kulkarni

Department of Mechanical Engineering

Indian Institute of Technology Bombay,Powai

Mumbai-400076 (INDIA)

December, 2020

Contents

Chapter 1

Pledge

I pledge on my honour that no part of this report or the MATLAB code is shared to or received by any of the coursemates. The entire work of the course project has been completely done by myself. I do accept that I have discussed some parts of the Pierre's paper [1] and verified my final answers with Saurabh Pal only over Phone call.

Chapter 2

Abstract

Eigen-value analysis of a complex structure is computationally expensive as it has many degrees of freedom. Component mode synthesis, treats a complex assembly as the assemblage of individual substructures. It transforms the coordinates of the structure/substructure to a new set of reduced coordinate system, thereby reducing the order of the system. Two such Component mode synthesis methods are Craig-Bampton and Characteristic constraint mode method. Craig-Bampton method [2] assumes the displacement of a substructure to be composed of constraint modes and normal modes. Each of these modes are obtained by applying different conditions on the boundary or the substructure interface degree of freedoms. Characteristic constrained method [1] performs eigen analysis on the partitions of the reduced order matrices of Craig-Bampton method corresponding to the constraint modes. Truncation of these characteristic constraint modes reduces the order of Craig-Bampton matrices even more. Each of these Characteristic constraint mode gives a principal way in which the interface can deform In this report, first 10 natural frequencies of a structure are determined using the above two methods, and the results are compared with the exact natural frequencies. Error analysis of the results obtained from the Characteristic constraint method is also done when different amount of truncation were made to the Characteristic constraint modes. With more number of Characteristic constraint modes considered, the results converge to the exact frequencies monotonically. Higher modes, are observed to have more error relative to the lower modes. Amount of error on a mode depends on how much the global mode is being captured by the considered Characteristic constraint mode.

Chapter 3

Introduction

A problem which requires to determine the first ten natural frequencies of a given structural assembly is solved. A direct method to determine the natural frequencies is by making use of the given assembled mass and stiffness matrices of the system. Since, an assembly has many degrees of freedom, it is often impractical to solve eigen-value problem of such large order matrices, as it would require great computational effort. Also, it is common for the substructures to be redesigned and analysed separately.

Component Mode Synthesis (CMS) is a class of method in dynamic sub-structuring, where the components or substructures are first reduced using a reduction bases and then assembled, using the continuity at the component interfaces. Depending on the reduction bases being used, there are various types of Component Mode Synthesis methods. The problem here is solved using the Fixed interface method or Craig-Bampton method. The solution is further improved by using the Characteristic-constrained modes as described in the paper by Pierre [1].

The columns of coordinate transformation matrix of either of these methods have different physical interpretations.

3.1 Objectives

The first 10 natural frequencies of the structure given below are determined using the Craig-Bampton Method [2] and Characteristic Constraint mode method [1]. The determined frequencies are compared with the frequencies found by solving the eigenvalue problem of the global mass and stiffness matrix without any reduction. Error analysis of the frequencies with respect to the considered number of characteristic modes is presented and discussed.

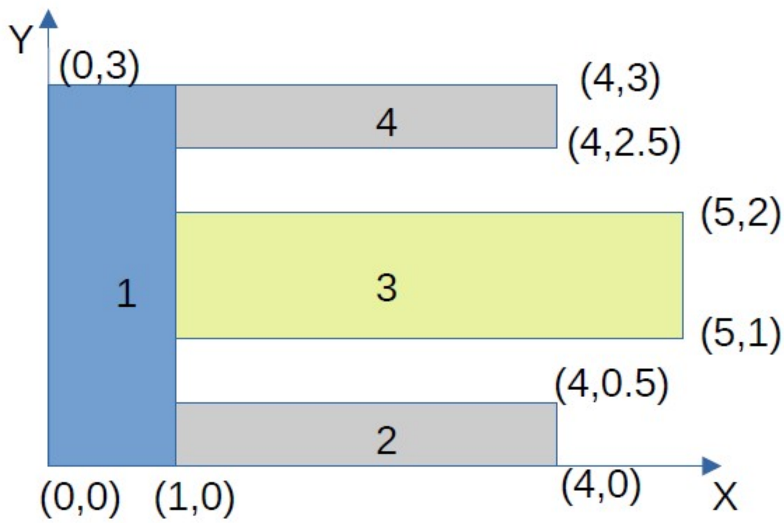

Figure 3.1: Assembled Substructure

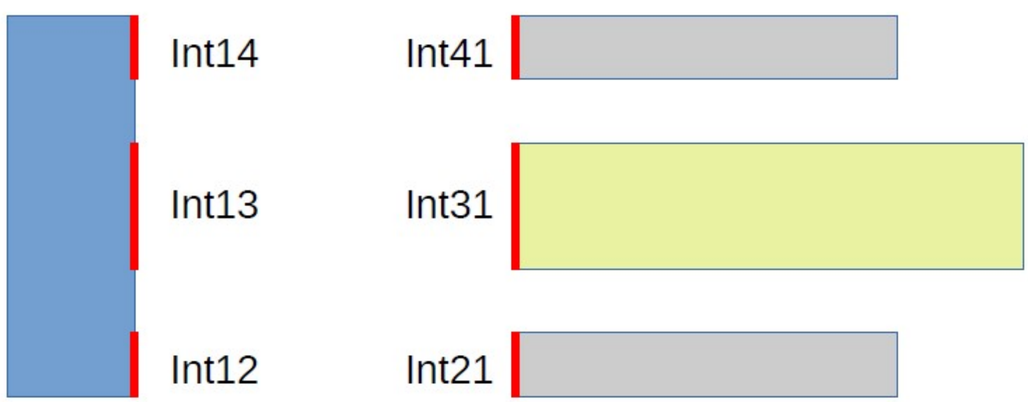

Figure 3.2: Substructures along with interfaces

The given mass and stiffness matrices of the substructures were assembled using the continuity conditions at the interface, and the Dynamic sub-structuring methods were then applied on those matrices.

3.2 Outline of the report

- **Methodology :-**

  The Craig-Bampton method [2] and Characteristic constraint method [1] are explained in this section, along with their advantages and drawbacks.

- **Results :-**

  The results of the problem solved using the above methods is presented in this section. The plots of the error analysis are also presented.

- **Observations and Discussions:-**

  The observations made in the presented results and plots are analysed and interpreted. Reasons for the mismatch with the exact results (frequencies) are interpreted and explained.

- **Conclusions:-**

  Based on the observations, conclusions are presented.

- **Appendix:-**

  The algorithm of the MATLAB code used to solve the problem is explained in this section.

Chapter 4

Methodology

4.1 Craig-Bampton Method

The Craig-Bampton method treats the response of the system being composed of constraint modes and normal modes. By introducing the new basis, comprising of the above modes, the coordinates of the reduced system consist of all the system boundary (interface) generalised coordinates and generalised coordinates due to substructure normal modes of all the substructures.

Craig-Bampton method separates the substructure degree of freedom into boundary and interface degree of freedom. Boundary degree of freedom corresponds to the nodes that are at the interface of the two substructures and also includes the nodes where external forces are applied. The remaining degrees of freedom are considered as internal degree of freedom. The substructure boundary is assumed to be completely constrained. The method starts with arranging the given substructure mass and stiffness matrices in the form as shown below :-

$$\begin{bmatrix} M^{BB} & M^{BI} \\ M^{IB} & M^{II} \end{bmatrix} \cdot \begin{bmatrix} \ddot{u}^B \\ \ddot{u}^I \end{bmatrix} + \begin{bmatrix} K^{BB} & K^{BI} \\ K^{IB} & K^{II} \end{bmatrix} \cdot \begin{bmatrix} u^B \\ u^I \end{bmatrix} = \begin{bmatrix} F^B \\ 0 \end{bmatrix} + \begin{bmatrix} g^B \\ 0 \end{bmatrix} \tag{4.1}$$

Where the superscripts B and I are boundary and internal degrees of freedom. F^B and g^B are external forces and interface reactions. The bases modes required for the reduction of the order of the substructure are determined as follows.

The constrained modes are defined as the mode shapes of the internal points, while successive unit displacements are given to the boundary points, with other boundary points being totally constrained. To determine these modes, all the dynamic (inertia) effects are ignored. Then,

$$u^I = -[K^{II}]^{-1}[K^{IB}]u^B \tag{4.2}$$

$$\Psi^C = -[K^{II}]^{-1}[K^{IB}] \tag{4.3}$$

The substructure normal modes, are the modes of the internal points, when all the boundary points are completely fixed. These modes can be found by solving the following eigen-value problem.

$$K^{II}\Phi = \omega^2 M^{II}\Phi \tag{4.4}$$

A reduction in the system order is made by not considering all the substructure normal modes. This gives us an observation that this method retains all the boundary degree of freedom, and causes the reduction in the internal degree of freedom.

A transformation matrix thus constructed using the basis modes will be,

$$R_{CB} = \begin{bmatrix} I & 0 \\ \Psi^C & \phi^N \end{bmatrix} \tag{4.5}$$

$$\begin{bmatrix} u^B \\ u^I \end{bmatrix} = R_{CB} \begin{bmatrix} u^B \\ u^N \end{bmatrix} \tag{4.6}$$

where ϕ^N is the truncation of the normal mode matrix. And,u^N's are the amplitudes of the considered normal modes. The reduced set of equation would then be,

$$\begin{bmatrix} M^{BB} & M^{BN} \\ M^{NB} & M^{NN} \end{bmatrix} \cdot \begin{bmatrix} \ddot{u^B} \\ \ddot{u^N} \end{bmatrix} + \begin{bmatrix} K^{BB} & K^{BN} \\ K^{NB} & K^{NN} \end{bmatrix} \cdot \begin{bmatrix} u^B \\ u^N \end{bmatrix} = R'_{CB} \begin{bmatrix} F^B \\ 0 \end{bmatrix} \tag{4.7}$$

or

$$M_r \ddot{u}_r + K_r u_r = \mathbf{R}'_{CB} \mathbf{F}_r \tag{4.8}$$

The reduced set of force vector can be obtained by the principle of virtual work, where the virtual work done by the force **F** in initial coordinates is equal to work done by the reduced set **P** in the reduced coordinates.Then,

$$\mathbf{P}_r = \mathbf{R}'_{CB} \mathbf{F}_r \tag{4.9}$$

The above set of equation 4.7 are substructure equations.

Once the reduced substructure matrices of all the substructures are obtained, these matrices can be assembled by imposing the continuity (compatibility) condition across the interfaces. Imposing the continuity conditions at various boundary degrees of freedom, would give us a set of compatibility equations and hence a transformation matrix representing those set of compatibility equations can be formed. This transformation matrix will assemble the sub-structures and express the equation of motion in terms of substructure normal modes, and generalised boundary coordinates.

Let the generalised boundary coordinates be represented in the vector u^B, and the substructure boundary degrees of freedom be represented by the vector u_r^B for the r^{th} substructure.u_r^N reperesents the normal mode coordinates for the r^{th} substructure. And ϕ_r^N represent the normal mode of r^{th} substructure. A general form of coordinate transformation relating the coordinates of all the substructures with the generalised boundary coordinates and the individual substructure normal mode coordinates,

$$\begin{bmatrix} u_1^B \\ u_1^N \\ \vdots \\ u_r^B \\ u_r^N \end{bmatrix} = [\beta] \begin{bmatrix} u_1^N \\ \vdots \\ u_r^N \\ u^B \end{bmatrix} \tag{4.10}$$

where $[\beta]$ is the transformation matrix.

If m and k are the mass and stiffness matrices, which have reduced substructure mass and stiffness matrices arranged along the diagonal, then they can be transformed into the assembled system as follows.

$$m = \begin{bmatrix} M_1 & 0 & . & . \\ 0 & M_2 & 0 & . \\ . & . & . & . \\ . & . & . & M_r \end{bmatrix} \tag{4.11}$$

$$k = \begin{bmatrix} K_1 & 0 & . & . \\ 0 & K_2 & 0 & . \\ . & . & . & . \\ . & . & . & K_r \end{bmatrix} \tag{4.12}$$

then, the final reduced equation would be

$$\mathbf{M}\ddot{u} + \mathbf{K}u = \mathbf{Q} \tag{4.13}$$

where

$$M = [\beta]' m [\beta] \tag{4.14}$$

$$K = [\beta]' k [\beta] \tag{4.15}$$

and

$$u = \begin{bmatrix} u_1^N \\ \vdots \\ u_r^N \\ u^B \end{bmatrix} \tag{4.16}$$

and

$$\mathbf{Q} = \begin{bmatrix} 0 \\ \vdots \\ 0 \\ F^B \end{bmatrix} \tag{4.17}$$

is the vector containing all the externally applied forces. The Craig-Bampton method simplifies the assembly process as it retains the interface degrees of freedom.

Drawbacks of Craig-Bampton

- The Craig-Bampton method, retains all the boundary degrees of freedom. All the order reduction is done in the internal degrees of freedom.
- For a large-scale structure, with many interfaces, a significant reduction in the order of the entire system, might not be achieved. This problem could be even more if the Finite Element mesh is sufficiently fine.

- Refining a finite element mesh, will increase the interface points and hence the order of the reduced system. The accuracy of the method depends upon the number of normal modes considered while forming the transformation matrix($\mathbf{R}_{CB}$. Mesh refinement will not have significant increase in accuracy of the final results.

Due to the above drawbacks, many developments have been made to the Craig-Bampton method, to cause a higher model order reduction. One of those method is the Characteristic Constraint modes method, explained in the following section.

4.2 Characteristic Constraint mode method

It is an improvement to the Craig-Bampton method [2], where the constraint modes from the Craig-Bampton method are replaced by the new set of modes called as the Characteristic constraint modes [1].

If the number of interface degree of freedom of a given substructure is N_Γ , which is determined by the finite element mesh, then there will be N_Γ number of constraint modes. This means a refined mesh would increase the number of constrained modes. With a large number of constraint modes, the individual constraint modes have limited physical meaning.

As explained in the work by Pierre [1], the significance of the constraint modes is explained here. Consider a two span beam as shown, in the figure 4.1. Let the FEM analysis of the beam be carried out seperately by Timoshenko beam element and linear hexahedral elements respectively.

For beam element FEM, there is only one degree of freedom at the interface (slope), and a unit angular displacement would give the constraint mode shape to beam 1, as shown in figure 4.1.

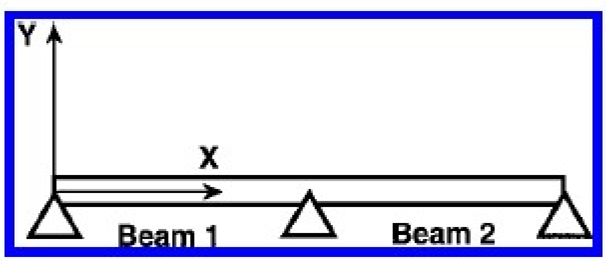

Fig. 1 Two-span beam on simple supports.

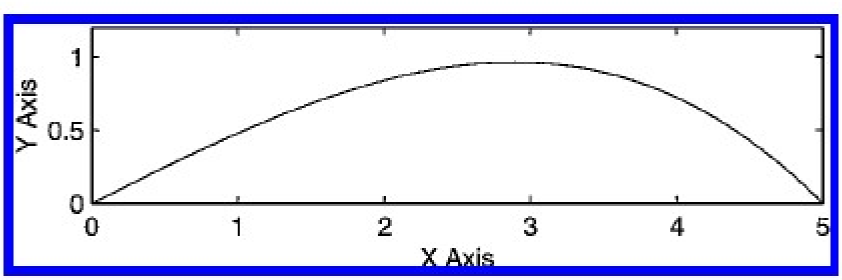

Figure 4.1: Two span beam and Single constraint mode of beam 1

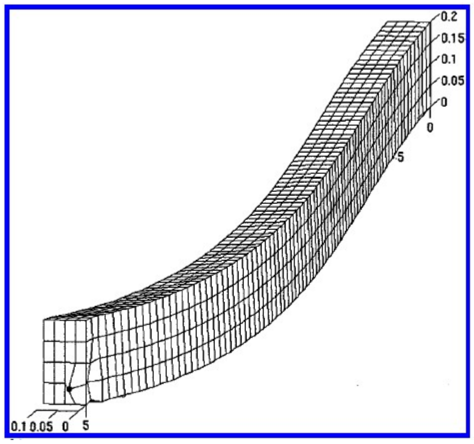

Figure 4.2: Beam with hexahedral element, interface at right end. One of the constraint modes of the solid element beam

For solid element FEM, as shown in figure 4.2 there are 20 unconstrained nodes at the interface, which means 60 degree of freedom, and hence 60 constraint modes. A linear combination of these similar constraint modes (where unit displacement is given in either x or y or z), would yield the shape, that is given by the single constraint mode of the beam element FEM model. A single constraint mode will then have a very limited physical meaning, since it alone will not produce significant deflections at internal points, as compared to the constraint mode of Beam element FEM.

The **idea of Characteristic constraint modes** is to look for a set of modes that can replace the constraint modes, and every individual mode of this set has a physical meaning attached to it. This means that every individual mode is a way in which the entire structure can deform. These modes do not give successive unit displacements to the interface, instead they give displacements to each and every interface node, and thereby give a set of principle ways in which the entire structure or substructure can deform. Ψ^Cs of individual substructures are taken into consideration, as they give relation between the internal and interface displacements. So, every characteristic mode has entries corresponding to each boundary and internal degree of freedom of the structure.

To proceed, we will first rearrange the reduced mass and stiffness matrices obtained from the Craig-Bampton method, as follows,

$$\begin{bmatrix} M^C & M^{C1} & . & . & M^{Cr} \\ M^{1C} & M^1 & 0 & 0 & 0 \\ M^{2C} & 0 & M^2 & 0 & 0 \\ . & . & . & . & \\ M^{rC} & 0 & 0 & 0 & M^r \end{bmatrix} \cdot \begin{bmatrix} \ddot{u}^B \\ \ddot{u}_1^N \\ \ddot{u}_2^N \\ . \\ \ddot{u}_r^N \end{bmatrix} + \begin{bmatrix} K^C & 0 & . & . & 0 \\ 0 & K^1 & 0 & 0 & 0 \\ 0 & 0 & K^2 & 0 & 0 \\ . & . & . & . & \\ 0 & 0 & 0 & 0 & K^r \end{bmatrix} \cdot \begin{bmatrix} u^B \\ u_1^N \\ u_2^N \\ . \\ u_r^N \end{bmatrix} = \begin{bmatrix} F^B \\ 0 \\ . \\ . \\ 0 \end{bmatrix} \tag{4.18}$$

Now, to find the characteristic constraint modes, we will start with solving the eigen-value problem,

$$K^C \Phi_{CC} = \lambda M^C \tag{4.19}$$

Equation 4.19 gives us the modes of vibration of the interface points, when the internal points are completely fixed. **This means that these are the possible ways in which the interface can move.**

The model order reduction can now be achieved by truncating the above eigen-modes. The reduced set thus obtained, can now be used to construct a transformation matrix. The transformation from the coordinates of the Craig-Bampton to characteristic constraint mode system,

$$\begin{bmatrix} u^R \\ u_1^N \\ u_2^N \\ . \\ u_r^N \end{bmatrix} = \begin{bmatrix} \phi^{CC} & 0 & . & . & 0 \\ 0 & I & 0 & 0 & 0 \\ 0 & 0 & I & 0 & 0 \\ . & . & . & . & \\ 0 & 0 & 0 & 0 & I \end{bmatrix} . \begin{bmatrix} u^B \\ u_1^N \\ u_2^N \\ . \\ u_r^N \end{bmatrix} \tag{4.20}$$

where ,

$$T_{CC} = \begin{bmatrix} \phi^{CC} & 0 & . & . & 0 \\ 0 & I & 0 & 0 & 0 \\ 0 & 0 & I & 0 & 0 \\ . & . & . & . & \\ 0 & 0 & 0 & 0 & I \end{bmatrix} \tag{4.21}$$

is the transformation matrix. Reduced mass and stiffness matrices can be obtained as,

$$M_{CC} = T'_{CC} M T_{CC} \tag{4.22}$$

$$K_{CC} = T'_{CC} K T_{CC} \tag{4.23}$$

The reduced eigen-modes obtained can be transformed into the FEM coordinates (the assembled mass and stiffness matrices obtained from FEM without any reduction) by,

$$\psi^{CC} = \begin{bmatrix} I \\ \Psi_1^C \\ \Psi_2^C \\ \vdots \\ \Psi_r^C \end{bmatrix} .\phi^{CC} \tag{4.24}$$

The ψ^{CC} obtained is called the **characteristic constrained mode**, and each of its column represents a mode in which the interface and thus a sub-structure or structure can move. Each column of ψ^{CC} shows the principle ways in which the structure can deform. If we denote the columns of ψ^{CC} as ψ_i^{CC}, then any global mode V can be written as

$$V = c_i \psi_i^{CC} \tag{4.25}$$

where the c_i's are the contribution(amplitudes) of the respective characteristic constrained modes.

So given the global matrices of a structure we can reduce it by Characteristic-constraint mode method as,

$$x = \begin{bmatrix} \phi^{CC} & 0 & . & . & 0 \\ \Psi_1^C \phi^{CC} & \phi_1^N & . & . & 0 \\ \Psi_2^C \phi^{CC} & 0 & \phi_2^N & . & 0 \\ . & . & . & . & . \\ \Psi_r^C \phi^{CC} & 0 & . & . & \phi_r^N \end{bmatrix} z \tag{4.26}$$

Where x is the FEM coordinate system and z is reduced coordinate system corresponding to the characteristic constraint mode.

An **advantage** of C**haracteristic constraint mode method** is that a refinement in Finite element mesh would increase the accuracy of the method, without requirung increase in the size of the final reduced order matrix, as same number of characteristic constraint modes can be retained

The first CC mode of the two span beam is shown in the figure 4.3 and it resembles with the first constraint mode of the timoshenko beam element.

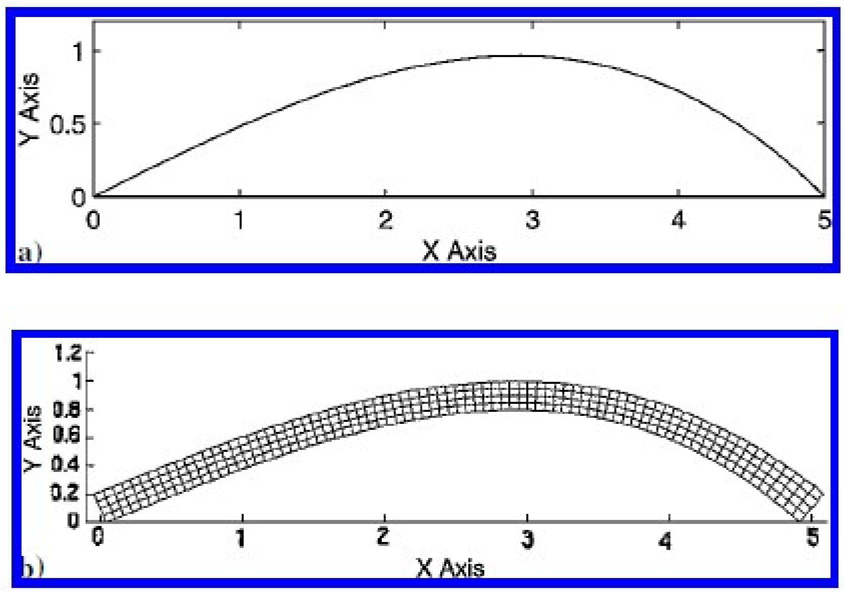

Figure 4.3: Comparison between Single constraint mode of the beam element and first CC mode of hexahedral element

Chapter 5

Results

- The given problem was solved using MATLAB (refer to appendix for code algorithm) after the substructure mass and stiffness matrices were assembled without any reduction.
- First the eigen-value problem of the assembled mass and stiffness matrices was solved to get first 10 natural frequencies.(ω_{actual})
- The global mass and stiffness matrices were then reduced using the Craig-Bampton method and eigen-value problem of the reduced system was solved.20 substructure normal modes were considered for each substructure.(ω_{CB})
- The mass and stiffness matrices thus obtained were further reduced using the transformation matrix of the Characteristic-constraint method. The eigen value of the reduced system was then solved.(ω_{CC})

The first 10 natural frequencies are tabulated below, for the case when 60 characteristic constraint modes were considered.

Actual(ω_{actual})	Craig-Bampton (ω_{CB})	Characteristic-constraint (ω_{CC})
0	0	0
0	0	0
0	0	0
4.4173	4.4176	4.4173
4.7051	4.7029	4.7051
12.1357	12.2912	12.1356
23.6055	23.5918	23.6057
26.5469	26.6012	26.5468
32.3998	32.9365	32.4003
34.2515	34.7143	34.2523

Frequencies using the Characteristic constraint mode method were determined by considering various number of Characteristic constraint modes ranging form 5 to 60. Error analysis was carried out to analyse the behavior of Characteristic constraint modes, in which;

- ω_{CC} was compared with ω_{actual}

- ω_{CC} was compared with ω_{CB}

The following plots show percentage error against the number of characteristic constraint modes considered. Since, the first 3 eigenvalues are zeros, they are not plotted.

5.0.1 ω_{CC} compared with ω_{actual}

$$percentageerror = \frac{\omega_{actual} - \omega_{CC}}{\omega_{actual}} x100 \tag{5.1}$$

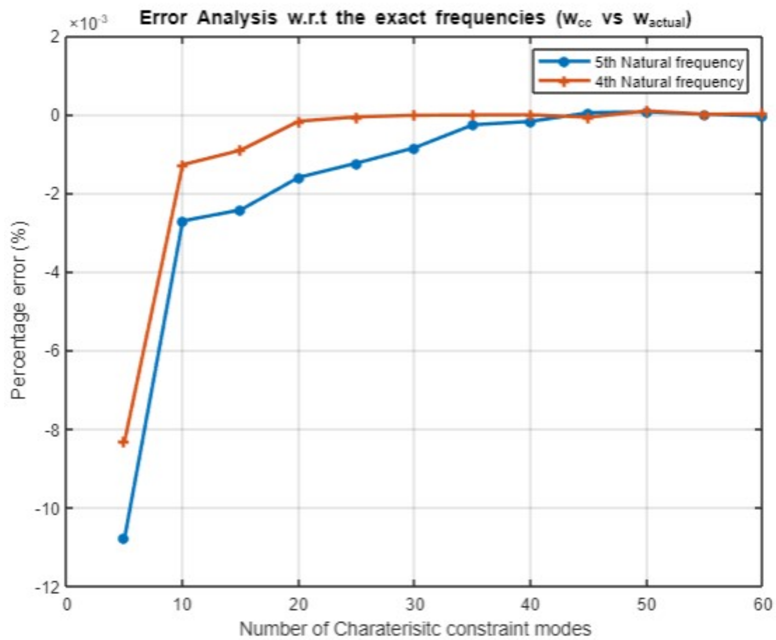

Figure 5.1: Error relative to actual 4^{th} and 5^{th} frequencies

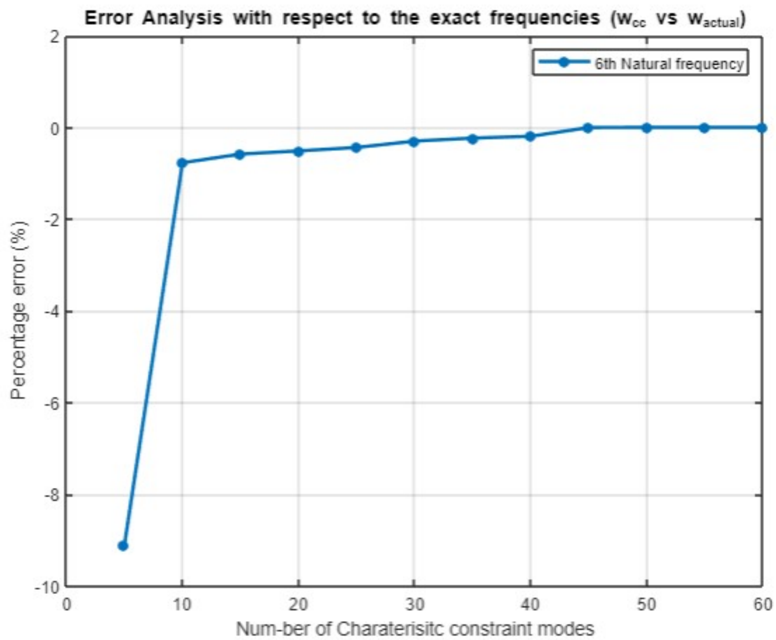

Figure 5.2: Error relative to actual 6^{th} frequency

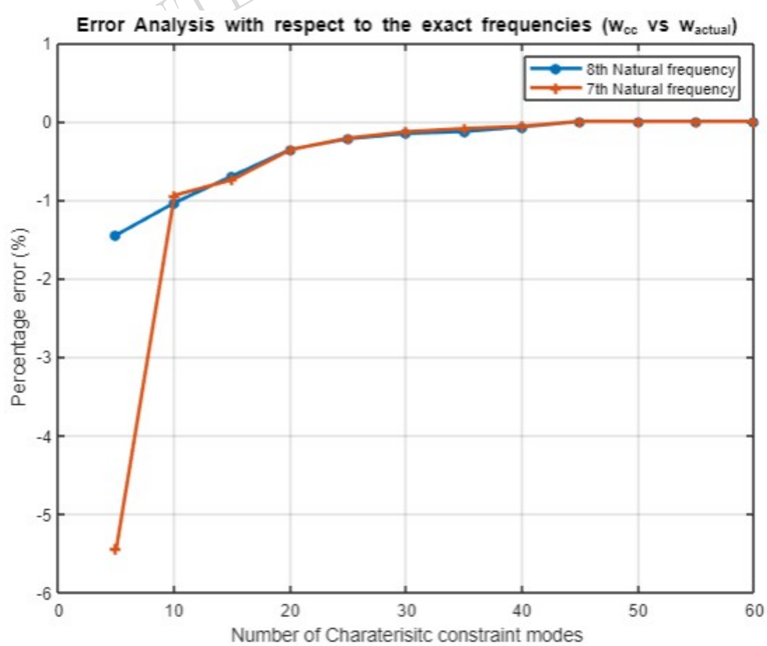

Figure 5.3: Error relative to actual 7^{th} and 8^{th} frequencies

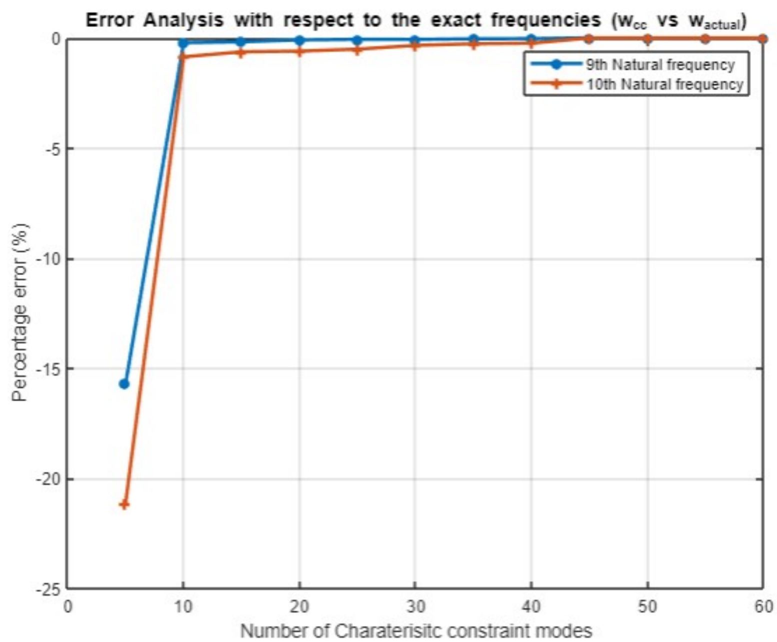

Figure 5.4: Error relative to actual 9^{th} and 10^{th} frequencies

5.0.2 ω_{CC} compared with ω_{CB}

$$percentage error = \frac{\omega_{CB} - \omega_{CC}}{\omega_{CB}} x100 \tag{5.2}$$

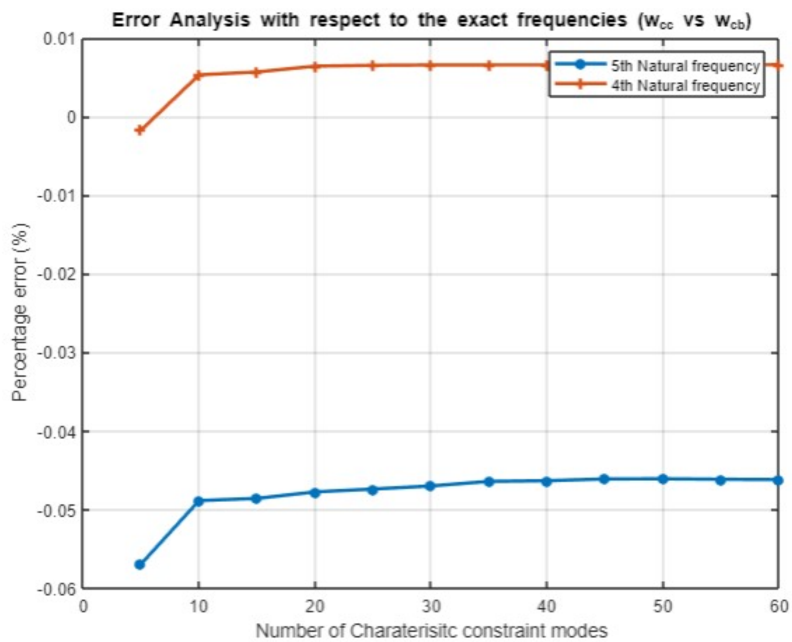

Figure 5.5: Error relative to actual 4^{th} and 5^{th} frequencies

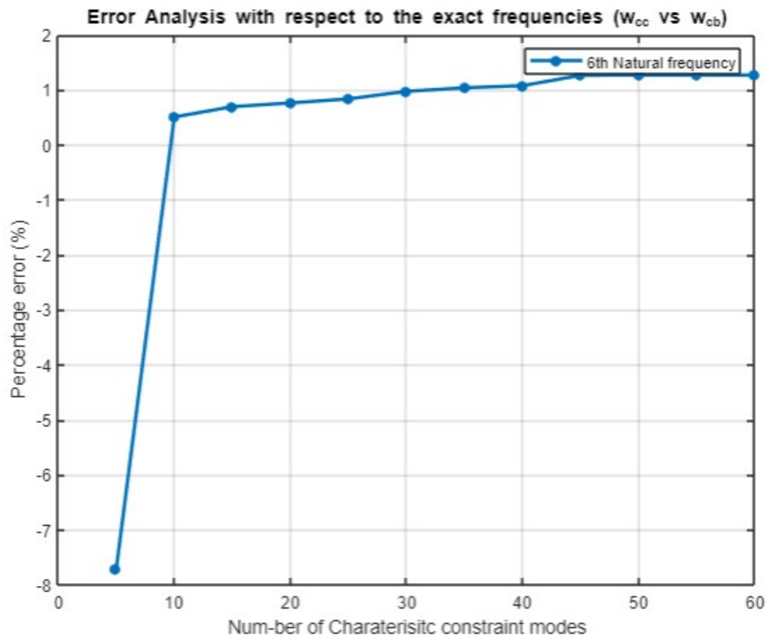

Figure 5.6: Error relative to actual 6^{th} frequency

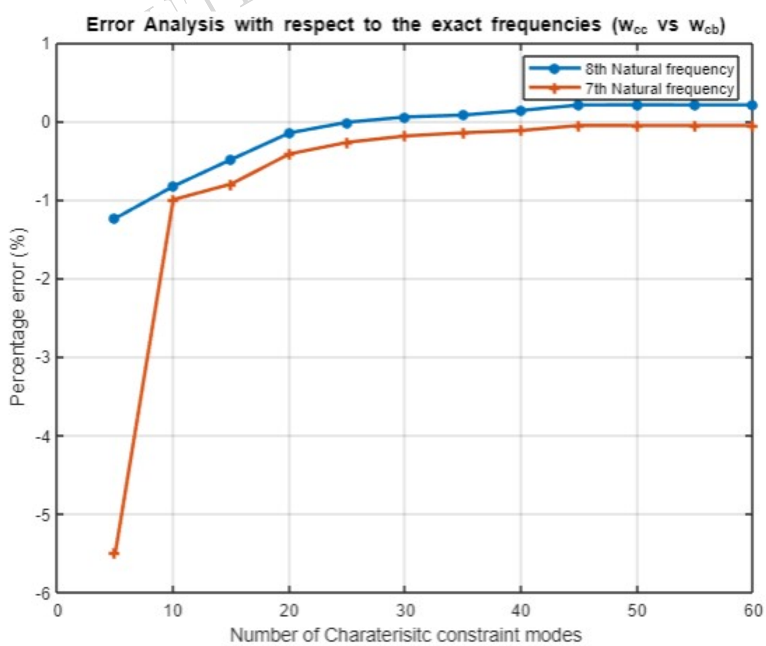

Figure 5.7: Error relative to actual 7^{th} and 8^{th} frequencies

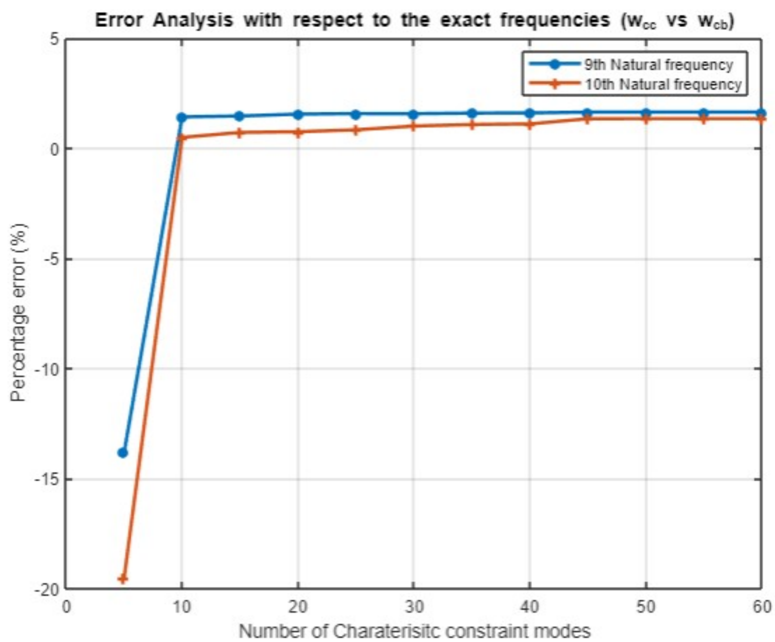

Figure 5.8: Error relative to actual 9^{th} and 10^{th} frequencies

Chapter 6

Obervations and Discussions

- The tabular representation of frequencies show that the Characteristic constraint mode method (ω_{CC}) is giving frequencies closer to actual value (ω_{actual}).
- The frequencies from the Craig-Bampton method (ω_{CB}) have more deviation from ω_{actual}.

Observations and Analysis of the two sets of plots shown above are presented below:-

- **ω_{cc} compared with ω_{actual}**
  - **Observations:-**
    * The percentage error in higher modes is more relative to the lower modes.
    * All the curves achieve convergence, after about 40 characteristic constraint modes are considered.
    * Rate of convergence is maximum between the first 5^{th} and 10^{th} characteristic constraint mode.
    * Percentage error for 8^{th} mode is least among 6^{th} to 10^{th} natural mode, when 5 characteristic constraint modes are considered.
    * Rate of convergence of 7^{th} and 8^{th} mode is almost same after 10 characteristic constraint modes are considered.
    * The percentage error in 4^{th} and 5^{th} natural frequency is relatively very low even when the considered characteristic constraint modes are less than 10.
  - **Discussions**:-
    * A higher percentage error in higher modes, might be because the higher global modes are not captured accurately by less number of characteristic constraint modes.
    * More than 40 characteristic constraint modes are sufficient to capture all the 10 global modes, this is the possible reason behind the convergence.
    * Let's consider any global mode, we can represent that global mode as a linear combination of these 60 characteristic constraint modes. The contribution (amplitude) of first 10 characteristic constraint modes

will be relatively higher than other modes. This is the reason behind great reduction in percentage error between first 5 to 10 characteristic constraint modes.

  * Less percentage error in the 8^{th} natural frequency shows that the contribution of first 5 to 10 characteristic modes, in constituting this mode is less than their respective contributions in the constitution of global mode 7.
  * The respective contributions (amplitudes) of the 10^{th} to 60^{th} characteristic modes are almost same in the formation of 7^{th} and 8^{th} global mode. This is the possible reason behind their same rate of convergence.
  * Linear combination of few initial characteristic modes provide a good enough approximation of the 4^{th} and 5^{th} global modes.
  * The plots show that the Characteristic constraint method is overestimating the natural frequencies until it converges to the exact value.

- ω_{CC} **compared with** ω_{CB}:-
  - **Observations :-**
    * Percentage error of none of the plot converges to zero, although with increasing number of characteristic modes, it does converges to a constant percentage error.
    * Behavior of 8^{th} natural frequency is similar to that of the previous case (ω_{cc} compared with ω_{actual}).
    * Rate of convergence is high while considering the initial 5 to 10 characteristic modes.
    * **Discussions :-**
      · Since the natural frequencies obtained by the Craig-Bampton method are not equal to actual frequencies, it is not expected for the plot to converge to zero.
      · Convergence indicates that linear combination of characteristic modes tend to represent a mode which is close to that represented by the linear combination of constraint modes of Craig-bampton method.
      · Looking at the figures 5.3 and 5.2, we cannot make a general comment that the percentage error is higher for higher modes.

6.1 Conclusions

- Careful selection of Characteristic constraint mode can lead to a more reduced model and close to accurate frequencies. The selected modes should have a greater contribution (amplitude) in the constitution of global deformation modes. For eg., In the above solved problem, if the Characteristic constrained modes considered for the formation of the transformation matrix are between 30 and 50, then the results obtained won't be very close to the exact results. This is because, these modes do not have significant contribution in constituting the global deformed mode.

- With 60 Characteristic constraint modes considered, the order of the system was 140x140. With 20 substructure normal modes being considered in the Craig-Bampton method, the order of the system was 166x166. Looking at the tabular results, the Characteristic constraint method gives more accurate results with an added advantage of analysis of a more reduced order.

- Varying the number of substructure normal modes in the Craig-Bampton method has no effect on the accuracy of Characteristic constraint mode method.

- Considering up-to 40 characteristic modes, would give close to same results. And even more reduced model.

- Figure 5.1 and figure 5.5 show that, lower modes are being captured reasonably well by both the methods. Either of the methods will give correct results, if one is concerned with the lower modes.

Chapter 7

Appendix

7.1 Algorithm

1. Arrange the given substructure mass and stiffness matrices in the following form

$$M_{asm} = \begin{bmatrix} M^1 & 0 & 0 & 0 \\ 0 & M^2 & 0 & 0 \\ 0 & 0 & M^3 & 0 \\ 0 & 0 & 0 & M^4 \end{bmatrix} \tag{7.1}$$

$$K_{asm} = \begin{bmatrix} K^1 & 0 & 0 & 0 \\ 0 & K^2 & 0 & 0 \\ 0 & 0 & K^3 & 0 \\ 0 & 0 & 0 & K^4 \end{bmatrix} \tag{7.2}$$

   where M^i, K^is are the substructure matrices.

2. Now use the interface continuity conditions to assemble the substructure matrices. We will use following coordinate transformation.

$$\begin{bmatrix} u_i^1 \\ u_b^{12} \\ u_b^{13} \\ u_b^{14} \\ u_i^2 \\ u_b^{21} \\ u_i^3 \\ u_b^{31} \\ u_i^4 \\ u_b^{41} \end{bmatrix} = \begin{bmatrix} I & 0 & 0 & 0 & 0 & 0 & 0 \\ 0 & 0 & 0 & 0 & I & 0 & 0 \\ 0 & 0 & 0 & 0 & 0 & I & 0 \\ 0 & 0 & 0 & 0 & 0 & 0 & I \\ 0 & I & 0 & 0 & 0 & 0 & 0 \\ 0 & 0 & 0 & 0 & I & 0 & 0 \\ 0 & 0 & I & 0 & 0 & 0 & 0 \\ 0 & 0 & 0 & 0 & 0 & I & 0 \\ 0 & 0 & 0 & I & 0 & 0 & 0 \\ 0 & 0 & 0 & 0 & 0 & 0 & I \end{bmatrix} \cdot \begin{bmatrix} u_i^1 \\ u_i^2 \\ u_i^3 \\ u_i^4 \\ u_b^{12} \\ u_b^{13} \\ u_b^{14} \end{bmatrix} \tag{7.3}$$

   The u_b^{ij} indicates the interface between i^{th} and j^{th} substructure. Using this transformation matrix, we will get the assembled mass and stiffness matrices without any order reduction method being applied.

3. Now arrange the mass and stiffness matrices in the form given in Pierre's work for simplicity, using the following transformation matrix.

$$\begin{bmatrix} u_i^1 \\ u_i^2 \\ u_i^3 \\ u_i^4 \\ u_b^{12} \\ u_b^{13} \\ u_b^{14} \end{bmatrix} = \begin{bmatrix} 0 & 0 & 0 & I & 0 & 0 & 0 \\ 0 & 0 & 0 & 0 & I & 0 & 0 \\ 0 & 0 & 0 & 0 & 0 & I & 0 \\ 0 & 0 & 0 & 0 & 0 & 0 & I \\ I & 0 & 0 & 0 & 0 & 0 & 0 \\ 0 & I & 0 & 0 & 0 & 0 & 0 \\ 0 & 0 & I & 0 & 0 & 0 & 0 \end{bmatrix} . \begin{bmatrix} u_b^{12} \\ u_b^{13} \\ u_b^{14} \\ u_i^1 \\ u_i^2 \\ u_i^3 \\ u_i^4 \end{bmatrix} \tag{7.4}$$

4. SOlve the eigen-value problem of the formed mass and stiffness matrices to determine the actual natural frequencies (ω_{actual}).

5. To apply the Craig-Bampton method, we need to construct the transformation matrix.For that, we need to determine the constraint modes, of all the substructures, and combine them with the component normal modes of all the substructures. This can be done on the assembled matrices as follows. The assembled stiffness matrix formed in previous step can be written in the form

$$K = \begin{bmatrix} k_{12,12} & k_{12,13} & k_{12,14} & k_{12,1} & k_{12,2} & 0 & 0 \\ k_{13,12} & k_{13,13} & k_{13,14} & k_{13,1} & 0 & k_{13,3} & 0 \\ k_{14,12} & k_{14,13} & k_{14,14} & k_{14,1} & 0 & 0 & k_{14,4} \\ k_{1,12} & k_{1,13} & k_{1,14} & k_1 & 0 & 0 & 0 \\ k_{2,12} & 0 & 0 & 0 & k_2 & 0 & 0 \\ 0 & k_{3,13} & 0 & 0 & 0 & k_3 & 0 \\ 0 & 0 & k_{4,14} & 0 & 0 & 0 & k_4 \end{bmatrix} \tag{7.5}$$

where k_is indicate the stiffness matrix partition of the respective substructures corresponding to the respective internal degrees of freedom. $k_{12,12}$ and similar submatrices indicates the stiffness matrix partition corresponding to the respective boundary(interface) degrees of freedom.

6. The transformation matrix of the Craig-Bampton method would then be,

$$R_{CB} = \begin{bmatrix} I_{12,12} & 0 & 0 & 0 & 0 & 0 & 0 \\ 0 & I_{13,13} & 0 & 0 & 0 & 0 & 0 \\ 0 & 0 & I_{14,14} & 0 & 0 & 0 & 0 \\ \psi_{1,12} & \psi_{1,13} & \psi_{1,14} & V_1 & 0 & 0 & 0 \\ \psi_{2,12} & 0 & 0 & 0 & V_2 & 0 & 0 \\ 0 & \psi_{3,13} & 0 & 0 & 0 & V_3 & 0 \\ 0 & 0 & \psi_{4,14} & 0 & 0 & 0 & V_4 \end{bmatrix} \tag{7.6}$$

where V_is are the truncated component normal modes of the respective i^{th} substructures. And $\psi_{i,jk}$ are the constraint modes of the i^{th} substructure in relation to jk^{th} interface. These can be determined as follows :-

$$k_i V_i = \lambda_i m_i V_i \tag{7.7}$$

$$\psi_{i,jk} = -k_i^{-1} k_{i,jk} \tag{7.8}$$

7. The assembled mass and stiffness matrices are then transformed using R_{CB} to form M_{CB} and K_{CB}.The eigen-value problem of K_{CB} and M_{CB} is solved which gives frequencies due to Craig-Bampton method (ω_{CB}).

8. To proceed to Characteristic-constraint mode method, we will solve the eigen-value problem of the interface degree of freedom partition of the mass and stiffness matrices (K^C and M^C), as explained in the methodology section. The formed transformation matrix (T_{CC})will then be used to transform K_{CB} and M_{CB}. The eigen value problem then solved will give us ω_{CC}.

Bibliography

[1] M. P. Castanier, Y.-C. Tan, and C. Pierre, "Characteristic constraint modes for component mode synthesis," *AIAA Journal*, vol. 39, no. 6, pp. 1182–1187, 2001.

[2] R. R. CRAIG and M. C. C. BAMPTON, "Coupling of substructures for dynamic analyses.," *AIAA Journal*, vol. 6, no. 7, pp. 1313–1319, 1968.